

The Tearing Test as a Means for Estimating the Ultimate Properties of Rubber

J. GLUCKLICH, *Technion, Israel Institute of Technology, Haifa, Israel, and Jet Propulsion Laboratory, Pasadena*, and R. F. LANDEL, *Jet Propulsion Laboratory, Pasadena, California 91103*

Synopsis

SBR, unfilled and filled with glass beads, MT, and HAF carbon blacks, was tested for tearing energy, rupture values in simple tension, tear diameter, and strain distribution at four rates and seven temperatures. The energy density to failure at the tear zone W_t was obtained from the tearing energy τ and the natural tear diameter d using a modified Rivlin and Thomas relationship $W_t \approx \tau/d$. This was then compared with the nominal energy density at rupture in simple tension W . It is shown that always $W_t > W$ (sometimes $W_t/W = 10$), that W_t is subject to a smaller statistical scatter than W , and that W_t is more amenable to the WLF type of superposition than W . It is concluded that W_t and not W is the strength-determining property. Where W data permitted superposition, it followed the WLF equation. It is presumed that so would W_t . τ , although more superposable than W , showed a bigger shift factor than that dictated by WLF, the difference being the result of the temperature dependence of the diameter. The reinforcing effects of the various fillers are also discussed. It is shown that the carbon black fillers increase both W_t and d . Glass beads have only a small effect on d and none on W_t .

INTRODUCTION

The uniaxial stress-strain curve of rubber as obtained from the simple tension test of either rings or dumbbell-shaped samples does not represent the entire behavior of the material up to failure. Since the material, in particular, crystallizing or filled rubber, is capable of sustaining stable cracks (examination by stretching of such sample after failure reveals the presence of numerous nicks that had formed during testing but had not propagated catastrophically), it is clear that stress and strain ahead of these cracks are much higher than the values measured at the sample's boundaries. Contrary to more rigid materials, for rubber there is no guaranteed way of computing the stress or strain concentration at the onset of tearing by the use of elastic formulae such as that of Inglis, for example. However, the knowledge of the entire range of behavior right up to failure is important for various purposes (such as for predicting failure, for investigation the effect of rate and temperature on it, or for the understanding of the reinforcing mechanisms of fillers). One way of looking closely at the near-ultimate behavior of the material is by conducting a tearing test such as the familiar "trousers" test. In contrast to the conventional tension test, the tearing test provides a quantity, i.e., the tearing force, which is a manifestation of events occurring at the fracture

zone. Unfortunately, this force cannot be interpreted explicitly in terms of the critical stresses or strains at that zone, due to the uncertainty with regard to the distribution of these quantities. However, a fairly accurate estimate of the energy density at the tear zone may be made. This value may then be compared with the nominal energy density in a uniformly tensioned sample to show how limited in extent the latter test is.

THE TEARING TEST

Rivlin and Thomas¹ derived the expression for the tearing energy τ (defined as the energy expended irreversibly for a tear of unit length). They used a criterion for tearing similar to the Griffith criterion for an elastic brittle material. This was

$$-\left(\frac{\partial E}{\partial c}\right)_l = \tau h \quad (1)$$

where E is the elastically stored energy density, c is the length of the tear, h is the thickness, and l is the loading machine grip separation. For a "trousers" type sample, they arrived at the relation

$$-\tau h = \left(\frac{\partial E}{\partial c}\right)_l = \left(\frac{\partial E}{\partial c}\right)_F - 2\lambda F \quad (2)$$

where F is the force needed to maintain tearing and λ is the extension ratio at the two legs. Since $(\partial E/\partial c)_F$ is the change in the stored energy due to the transference of a unit length of the sample from the nonstretched to the stretched state, this term may be neglected in cases of sufficiently wide samples when, in addition, λ may be approximated to 1. In such cases, therefore,

$$\tau = 2F/h \quad (3)$$

from which the tearing energy may be very conveniently obtained by means of the force F . Experience shows that this force is not uniform and the force-tear diagram has considerable fluctuations. Since eq. (1) is a criterion for instability, the value of F to be used in eq. (3) must be the force at instability or the peaks of the force-tear diagram. In practice, the mean of all the peaks is used.

Thomas² has postulated the relationship

$$\tau \approx Wd \quad (4)$$

where W is the energy input to break in uniaxial tension and d is the effective tear diameter or the "bluntness" offered by the tear, which tends to deviate laterally. He proved the validity of eq. (4) by making incisions of varying tip diameter and measuring the corresponding tearing energies. He showed τ/d to be fairly constant and approximately equal to W as obtained from uniaxial tension tests. Actually, his τ/d values were about 20% higher than W , but he ascribed the difference to a size effect, the tension sample being much larger than the tensional zone in the tearing sample.

Greensmith,³ in a similar work, took account of the relative strain velocities in the two types of test. If the tearing rate is R and the uniaxial strain rate ahead of the tear is V , then the relation between the two values is

$$R \approx AVd \left[A = \frac{r_0/d}{\lambda - 1} \right] \quad (5)$$

where r_0 is the distance from the tear front of the point at which the strain decays to zero and λ is the extension ratio at the root of the tear. A is a dimensionless coefficient; Greensmith determined its value empirically and found it equal to 0.75. The simple tension data at the extension rate V is to be compared to the tearing data at the tearing rate R .

EXPERIMENTAL

Materials

SBR-1500 was used throughout. The fillers and their loadings ϕ (in vol-%) were as follows: series A, glass beads ($\phi = 0, 10, 20, 30, 40$); series B, MT carbon black ($\phi = 0, 10, 20, 30, 40$); series C, HAF carbon black ($\phi = 0, 10, 20, 25, 30, 35$).

The formulations and the physical details of the fillers appear in the appendix.

Samples

Four types of samples were used, all approx. 2 mm thick:

(i) **Tearing Samples.** These were the regular trouser samples of 12.5-cm length, 3.8-cm width, and having a razor-made 5.0-cm-long incision in mid-width. (In some cases a double sample, i.e., with two symmetrically spaced incisions, was used instead. This gave the sample better stability and reduced the load fluctuations somewhat.)

(ii) **Tension Samples.** These were rings of the nominal dimensions 1.91-cm I.D. and 2.22-cm O.D., cut from the molded sheets by means of a specially designed four-blade cutter mounted in a high-speed mill.

(iii) **Tear Diameter Samples.** To determine the natural tear diameter for every mix at the various rates and temperatures, special tearing samples with perfectly circular holes of desired diameters were vulcanized in specially designed molds (Fig. 1). The hole diameters varied from 0.1 to 1.0 mm in 0.1-mm intervals and from 1.0 to 9.0 mm in 1.0-mm intervals. They were formed by inserting pins of desired diameters through the unvulcanized material during vulcanization, typically about 5 min after heating started. The samples were smaller than the regular tearing samples: 2.9 cm long and 1.75 cm wide, and had a 2.0-cm-long incision ending at the hole so that the tear had to begin from the hole when the legs were pulled apart. When attached to the Instron, these samples were gripped close to the holes so that the onset of tearing would be distinctly marked on the chart by a point of maximum load or by a sudden change of slope (with long-legged samples the event of tear initiation would be obscured). Further details are given in Ref. 4.

(iv) **Strain Distribution Samples.** To determine the constant A in eq. (5); samples such as described by Greensmith³ were employed (see also ref. 4).

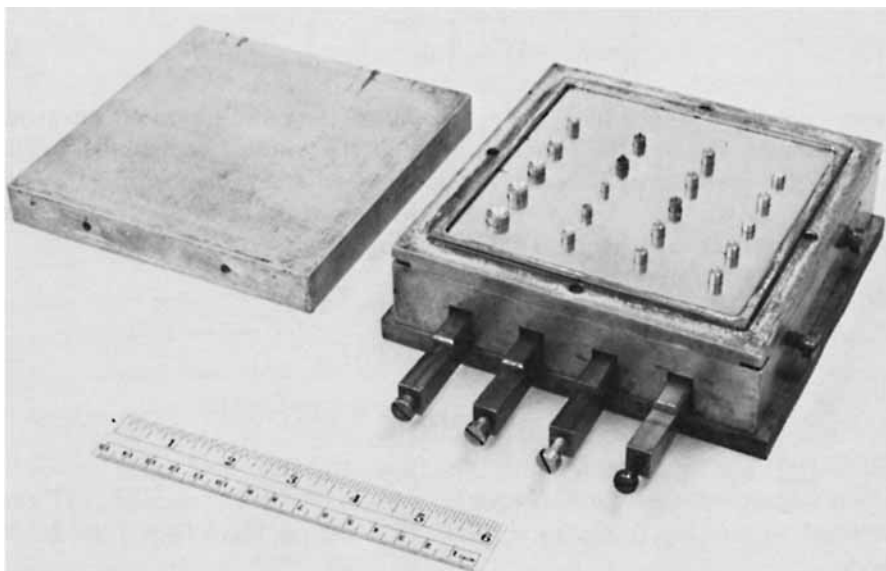


Fig. 1. Mold for tear-diameter samples.

Test Description

(i) **Tearing Tests.** These were run on the Instron in the regular fashion at the following four tearing rates R (the grip separation rate was twice the tearing rate): 0.01, 0.1, 1.0, 10 in./min (0.0254, 0.254, 2.54, 25.4 cm/min) and at the following seven temperatures: 233°, 253°, 273°, 293°, 313°, 333°, 353°K, making in all 28 test conditions. The value of F for eq. (3) was obtained by taking the arithmetic mean of all the peaks in the chart.

(ii) **Tension Tests.** These were also run on the Instron which was fitted with special metal hooks 1.0 cm in diameter. The cross-head rates were: 0.2, 2.0, 20, 200 in./min (0.508, 5.08, 50.8, 508 cm/min), which corresponded with strain rates V of 0.17, 1.7, 17, 170 min^{-1} , respectively. (For the highest speed, a special adjustment was made in the Instron.) These rates were adopted to enable correlation with the tearing rates R in accordance with eq. (5) and assuming d to vary between 0.05 and 0.5 cm. Tests were run at the forementioned 7 temperatures. Areas under the stress-strain curves obtained from these tests were used to compute W .

(iii) **Tear Diameter Tests.** These tests were run at only one out of the 28 test conditions: temperature of 293°K and rate of 1 in./min (2.54 cm/min) in series A and C; 0.1 in./min (0.254 cm/min) in series B. The test determined the force for initiating a tear from a given hole. Plots were then made of this force versus the hole diameter. Regular tear tests, i.e., tears initiating from razor blade incisions rather than from holes, on samples of identical dimensions, were then run to determine the mean tearing force F_s (the subscript indicates "small" samples, where $F_s \neq F$). When F_s was introduced into the forementioned plots, the natural tear diameter for the given material at the given test conditions could be read off. It was then assumed that this natural tear diameter was independent of the sample dimensions and was thus also applicable to the tear developing in the large size samples.

This test was in principle identical to that made by Thomas²; but, whereas Thomas made the holes by cutting into the vulcanized rubber, a method which must have nicked the cut surfaces causing stress concentrations far in excess of the intended ones, in the present work the circular surfaces were almost perfect. (Prior to making the holes in the molds, as just described, an attempt was made to drill holes in the vulcanized (and cooled down) material. However, the scatter of tearing forces obtained from such holes was about 10 times higher than that from molded holes. In fact, in some cases there was almost no correlation between the drilled hole size and the tearing force, indicating the nucleation of tears to be from random nicks within the nominal hole. Microscopic examination indeed revealed these nicks and also their absence in the molded holes. The authors concede the possibility of some anisotropy in the hole surface introduced during the vulcanization process.)

(iv) **Strain Distribution Tests.** Only two such tests (for mixes B-0 and B-30) were conducted by stretching the samples on a rack with one fixed and one traveling clamp. The extensions of marked lines, equally spaced away from the circular hole, were measured by means of a traveling microscope for the various extensions of the sample, and from this r_0 of eq. (5) was determined.

TEST RESULTS

Tearing Tests

The tearing behavior of the material, as manifested by the force-tear charts as well as by the tear surface, was of the three familiar types: steady, stick-slip, and knotty with the deviations, and hence d values, increasing in that order. In addition, a "smooth" tear, which is a knotty tear of a very large diameter, was observed. In such a case, only part of a single knot had a chance to form before the tear reached the edge of the sample. The types of tear are shown in Figure 2, and a detailed description is presented in Reference 4. The fluctuations observed in the tearing force, even in the steady type of tear, could be associated with varying effective tear diameter. Careful observation always revealed correspondence between high peaks in the force diagram and relatively large chunks of rubber pulled out of one leg of the sample and leaving a pit in the other.

The tearing energies derived from the tearing force were related to half the cross-head rate, although it was realized that the actual rate of tearing fluctuated within the cycle, reaching a minimum toward a peak and a maximum immediately following a peak.

Graphs were made (not shown) of τ versus ϕ for all rates and temperatures. These show for series A (glass) only a small increase of τ with ϕ but at a gradually increasing rate; for series B (MT) a small increase up to about $\phi = 20\%$ and a very sharp increase beyond it with a maximum somewhere between 35% to 40%; for series C (HAF), a similar behavior, but with a maximum at about 23% and a sharp drop beyond it. In all cases, stick-slip or knotty tears were observed whenever high τ values were reached, knotty tears being responsible for the highest values.

The same results were also presented in the form of three-dimensional plots with $\log \tau$ plotted versus T and $\log R$ with the aim of bringing out the

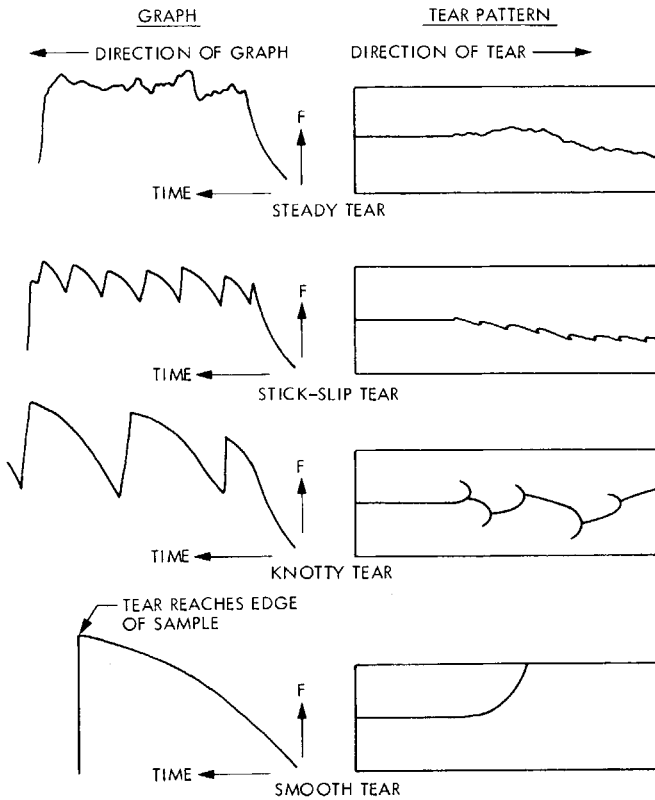


Fig. 2. Schematic representation of four types of tear.

contributions of temperature and rate. Such plots were made for each of the 16 material combinations, but Figures 3 through 5 show only the zero and optimum filler loadings of each material. The type of tear is also indicated on the τ surfaces.

Tension Tests

Values of W as obtained from the areas under the stress-strain curves were similarly plotted versus ϕ (as function of V) and, in three-dimensional plots, versus T and R . To save space, these are not shown here, but it should be mentioned that, as compared with their τ counterparts, the W plots show a much higher scatter.

Tear Diameter Tests

The F_s -versus- d curves were made for all mixes and the natural tear diameter determined for the specified combination of temperature and rate. Figure 6 is an example of such a curve. In view of eqs. (3) and (4), these curves might perhaps be expected to be linear, with slopes being measures of the energy density. However, the following two reasons could account for this not being so: (a) τ is proportional to F but not to F_s because of the geometrical

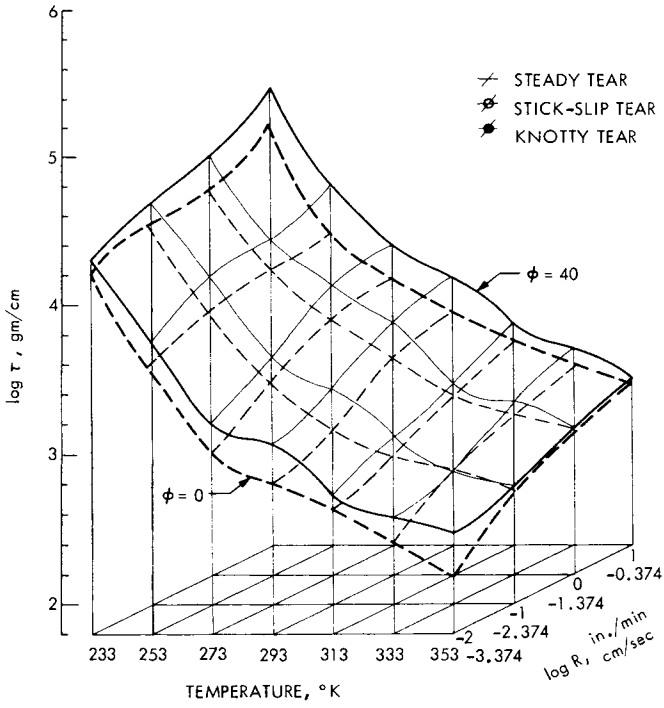


Fig. 3. Plot of τ - T - R for series A (glass) at zero and optimum filler loading.

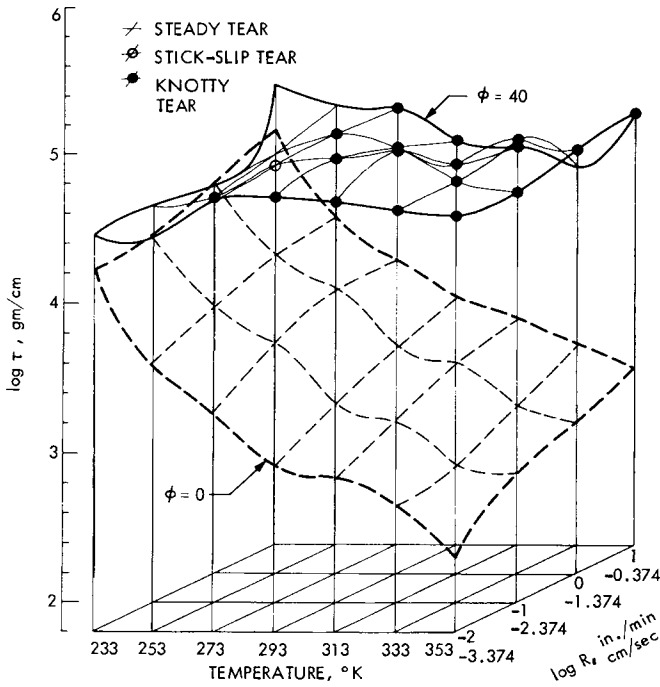


Fig. 4. Plot of τ - T - R for series B (MT) at zero and optimum filler loading.

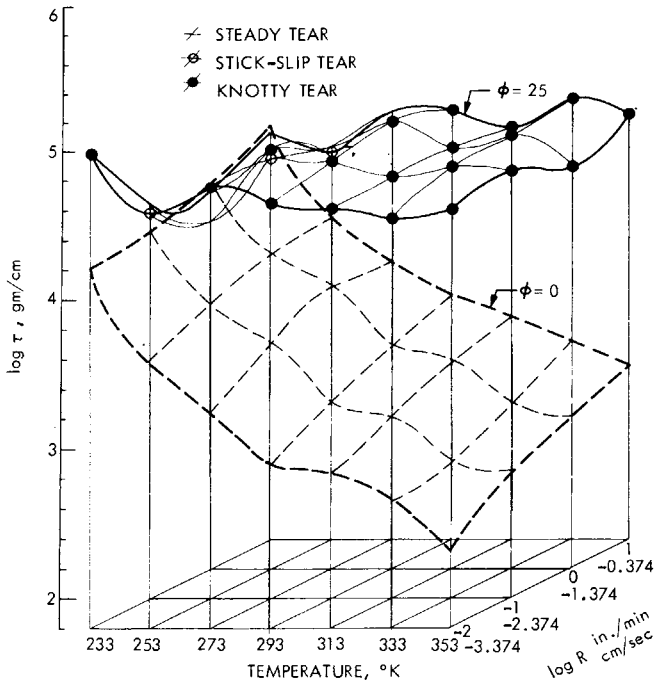


Fig. 5. Plot of τ - T - R for series C (HAF) at zero and optimum filler loading.

considerations involved in the derivation of eq. (3); (b) the strain rate varies with the size of the hole so that every point in such a curve represents a different rate. Consequently, this procedure should be viewed not as a means of obtaining directly the energy density at the tear zone, but rather as a "calibration" procedure from which the size of the natural tear is obtained from the force needed to tear holes of known sizes.

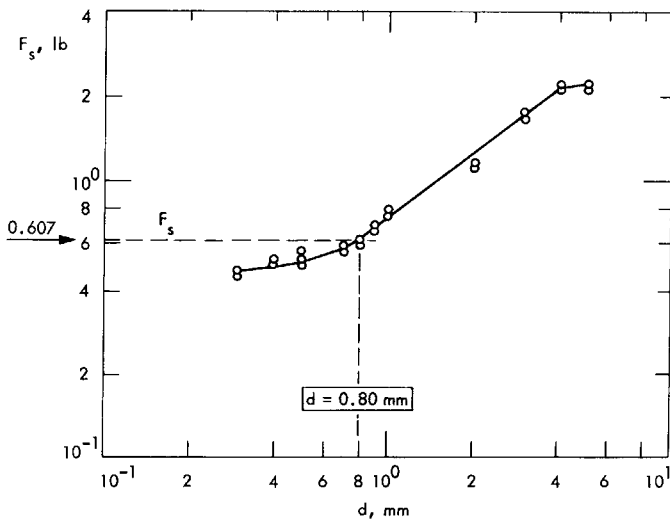


Fig. 6. Determination of diameter of a natural tear. Material A-30; $R = 1$ in./min; $T = 293^\circ\text{K}$.

The tearing energy τ which had been evaluated from the large tearing samples data (as previously described) was also derived from the small tearing samples using F_s values instead of F and the load-extension data obtained in the simple tension tests. The procedure followed the theory of Rivlin and Thomas¹ without the approximation requiring wide trouser legs. The ratio F/F_s averaged approximately 1.33, and the τ values were within 10% of their large sample counterparts, but some tendency for τ to decrease with the decreasing sample was indicated. Due to the small number of the "small" measurements, no statistical analysis was possible.

Strain Distribution Tests

The curves $\lambda-1$ versus r/d , used to determine the constant A , are not shown. In both B-0 and B-30 materials, a mean value of 0.85 was obtained for the constant A .

ANALYSIS AND DISCUSSION

Two categories of factors are involved in this work: (1) the filler, and (2) the test condition.

Effect of Filler on the Material Parameters

The effect of filler loading on the various material parameters are shown in Table I for all three series. Since d was obtained at only one test condition, the information in the table is confined to this condition. The parameters involved are as follows: τ , as measured by the tearing tests; d , as obtained from the "calibration" curves; W_t , being the energy density at the tearing

TABLE I
Effect of Filler Loading (ϕ) on Material Parameters^a

Series	R , cm/min	ϕ , %	τ , g/cm	d , cm	W_t (= τ/d), g/cm ²	V (= R/Ad), min ⁻¹	W , g/cm ²	k (= W_t/W)
A (Glass)	2.54	0	1,790	0.034	52,600	88.0	4,900	10.70
	2.54	10	1,540	0.065	23,700	46.0	5,200	4.55
	2.54	20	1,540	0.070	22,000	43.0	5,650	3.90
	2.54	30	2,020	0.080	25,300	37.0	5,450	4.65
	2.54	40	3,180	0.090	35,300	33.0	4,950	7.15
B (MT)	0.254	0	1,360	0.033	41,200	9.03	4,090	10.10
	0.254	10	5,200	0.095	54,700	3.14	11,960	4.58
	0.254	20	12,300	0.110	112,000	2.72	75,000	1.49
	0.254	30	61,000	1.000	61,000	0.30	60,200	1.02
	0.254	40	63,300	0.650	97,400	0.46	77,850	1.25
C (HAF)	2.54	0	2,060	0.036	57,200	83.0	6,160	9.28
	2.54	10	20,150	0.150	134,500	19.9	57,200	2.35
	2.54	20	49,600	0.165	300,000	18.1	180,000	1.67
	2.54	25	66,600	0.430	154,500	6.9	125,300	1.23
	2.54	30	35,300	0.285	124,000	10.5	74,040	1.67
	2.54	35	30,400	~0.200	~152,000	~15.0	~50,000	~3.04

^a Temperature = 293°K.

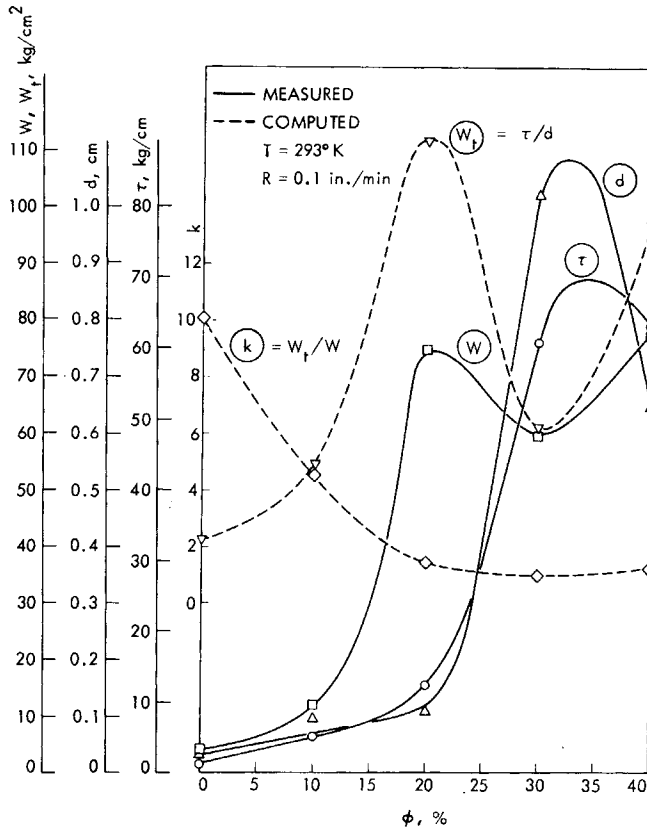


Fig. 7. Effect of the MT carbon-black filler concentration on the material parameters.

zone (and differentiated from W , the mean energy density), by use of the equation

$$\tau \approx W_t d \quad (6)$$

which is now offered to supersede eq. (4). (This was first suggested by Lake, Lindley and Thomas,⁵ but not pursued further.) Finally, W , as obtained from the simple tension tests. To be able to compare W against W_t , the two quantities should relate to the same strain rate. Therefore, the rate V was computed from the given R by the use of eq. (5) with $A = 0.85$ and d being the tear diameter corresponding to the respective filler loading. The W values corresponding to this V was then interpolated from the W -versus- ϕ curves as function of V (not shown) and entered in the table. Also included in the table is the energy concentration factor $k = W_t/W$. The above information as pertaining to the MT and HAF fillers is presented in graph form in Figures 7 and 8, respectively.

The first thing that comes to light is that in all cases $W_t > W$, i.e., as expected, the true input energy to break is higher than that measured in the simple tension test. Secondly, the dependence of k on d is also as it should be, with k showing a minimum in cases of knotty tears (maximum d values). Other points worth noting are:

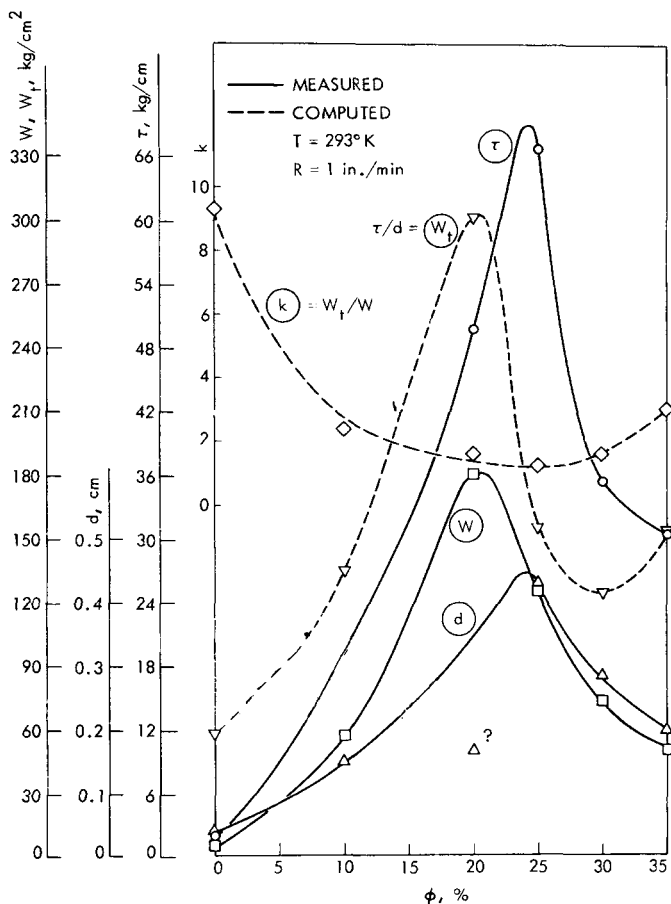


Fig. 8. Effect of the HAF carbon-black filler concentration on the material parameters.

(i) Glass beads, nonreinforcing fillers, have some reinforcing effect presumably by causing secondary microtears (or dewettings) in the tearing zone which is equivalent to blunting of the tear. The tear is only of the steady type.

(ii) MT and HAF carbon blacks have very strong reinforcing effect (in terms of tearing energy) which, contrary to some opinions,⁶ is the result of the increase of both the intrinsic strength (W_t) and the tear diameter, although the latter is predominant.

(iii) MT is as good a reinforcing filler as HAF but needs a higher filler loading (approx. 35% versus 25%) for optimum effect. The difference in behaviors may be due to the bigger size of the MT particles. (Actually, MT is probably a somewhat better reinforcer than HAF in view of the fact that the values for series B relate to a rate of 0.1 in./min while for series C to a rate of 1.0 in./min).

(iv) k is equal to 1.23 at $\phi = 25\%$ for the HAF material. This value is about the same as that reported by Greensmith³ for SRF-filled SBR (at the same loading and temperature) and was ascribed by him to a size effect. It is now clear that this cannot be so, for the following reasons: (1) Size effect has

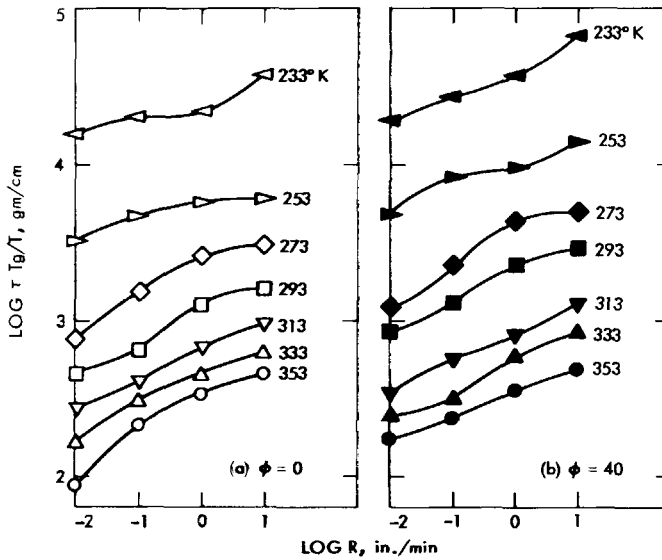


Fig. 9. Dependence of tearing energy τ on rate and temperature for series A (glass) ($T_g = 213^\circ\text{K}$).

to do with the distribution of flaws. While such distribution may indeed affect the failure values of whole samples, such as the present *tension* samples, it is of no consequence when the tear locality is predetermined by the presence of an incision, as in the present *tearing* samples. Size effect may account for differences in strength only between similar whole samples which vary only in size. (2) The table shows a strong dependence of k on the filler loading ϕ . Unless ϕ affects the size of the highly stressed zone ahead of the tear, and there is no indication of this, size effect cannot be the cause of this behavior. The observation $W_t > W$ made by Greensmith and by the present author is clearly the result of energy concentration at the tearing zone: In simple tension the energy density W is the mean value for the entire sample; in tearing, the energy density W_t is the peak value at the highly stressed zone. Also, in any simple tension test, W is the nominal density while W_t is the actual density reached at some locality where the tear actually developed.

(v) The curves in Figures 7 and 8 show quite interesting features which will not be discussed here. Mention will only be made of the following points: the W_t curves, in both the MT and the HAF materials, have a maximum, followed by a minimum; in both materials, these features occur at the same ϕ values; the W curves tend to follow the same pattern. In reference 4, this is discussed more fully in terms of dewetting versus interlocking of the filler particles and the relation of these mechanisms to the particles' size.

Effect of Temperature and Rate on the Parameters

The main thesis offered here is that W_t and not W is the material parameter. One way of checking this would be to try the rate-temperature equivalence principle on both these quantities. Unfortunately, W_t values are avail-

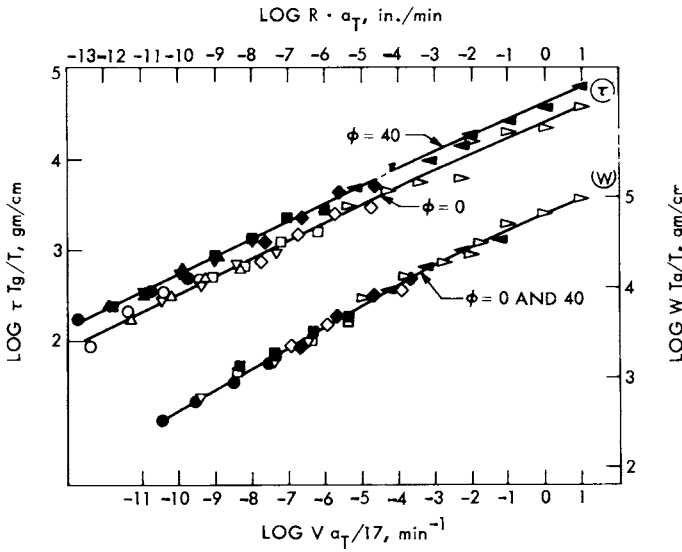


Fig. 10. Transformed tearing energy data for series A (glass).

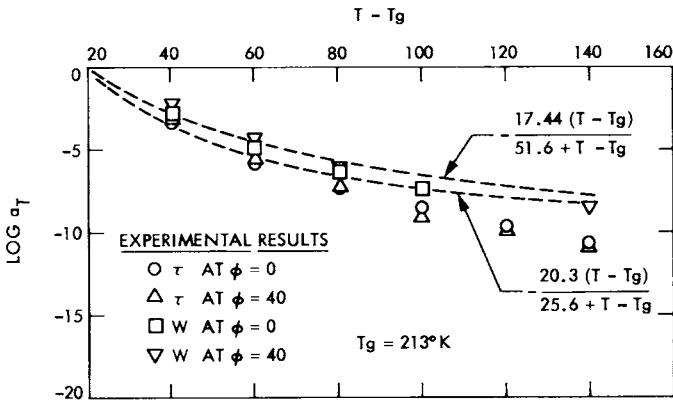


Fig. 11. Temperature dependence of the shift factors a_T in the cases of τ and W .

able for only one rate and one temperature (because of the similar limitations in *d*). The next best thing would be to try τ . Mullins,⁷ using data of Greensmith and Thomas, applied this principle to τ and, by shifting and superposing, obtained a master curve which indeed confirmed the equivalence of T and R . However, his a_T -versus- $(T - T_g)$ curve (where a_T is the shift factor and T_g is the glass transition temperature) was higher than the WLF curve by a factor of about 1.4. Mullins explained this discrepancy by assuming that both the input energy and the tear diameter, the two factors of the tearing energy, are rate and temperature dependent reflecting the viscoelastic nature of the rubber. Gent and Henry⁶ proved this assumption to be true by showing that the dependence of τ on T and R was exactly according to the WLF equation when tear deviations were prevented. When not prevented, they too obtained a dependence 1.4 times greater than the WLF.

In the present work, only in the case of series A was there a chance of ob-

taining a WLF type relationship for τ , because of the strong tear deviations in the carbon black materials. The raw data of materials A-0 and A-40 are shown in Figure 9, the transformed curves are in Figure 10 (upper two curves), and the temperature-dependence of the shift factors is in Figure 11. In the latter figure, the WLF equation

$$\log a_T = -C^{\circ}_1(T - T_0)/(C^{\circ}_2 + T - T_0)$$

was included. Here, T_0 was taken as the glass transition temperature T_g ($= 213^{\circ}\text{K}$), C°_1 and C°_2 were taken to be 20.3° and 25.6°C , respectively after

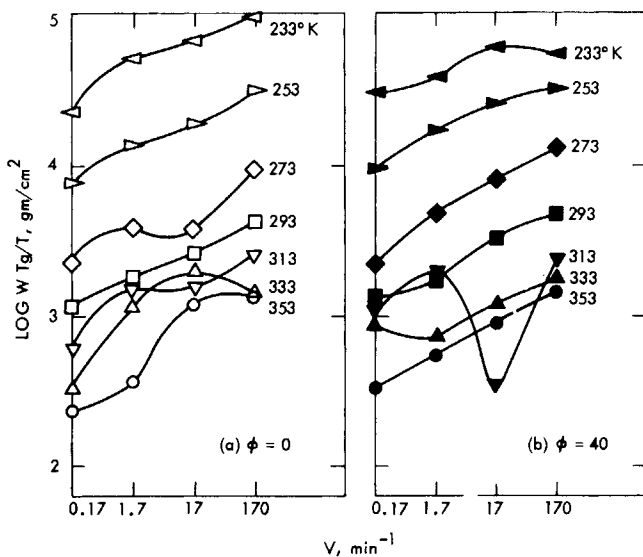


Fig. 12. Dependence of nominal input energy W on rate and temperature for series A (glass) ($T_g = 213^{\circ}\text{K}$).

Ferry.⁸ As can be seen, τ was found to be superposable although the shift factor was in this case 1.33 times greater than the WLF prediction. The conclusion must be similar to that of Mullins, i.e., that the tear diameter as well as the input energy is rate and temperature dependent although in an opposite sense: while the increasing rate increases the energy, it decreases the diameter by reducing the time available for deviations.

The rate-temperature superposition was then attempted for W . Again, A-0 and A-40 were used (other materials showed the same behavior) in Figure 12 to represent the rate and temperature dependence of W . It was immediately apparent that no superposition was possible due to the high scatter of W values.

The idea thus lends itself that τ is more fundamental than W . Actually, W_t is the fundamental property and W is merely an arbitrary fraction of it, whose magnitude depends on the statistics of various geometrical factors. The scatter of results in the measurements of W throughout this investigation supports this idea.

If W_t is the fundamental strength-determining property, it should not merely superpose easily but should also adhere to the WLF equation. This could not be checked in the present work but on the assumption that W , although only a fraction of W_t , is equally temperature and rate dependent, it was employed for this purpose *where the scatter permitted the operation*. Thus, in Figure 12a, all but the two higher temperatures, and in Figure 12b,

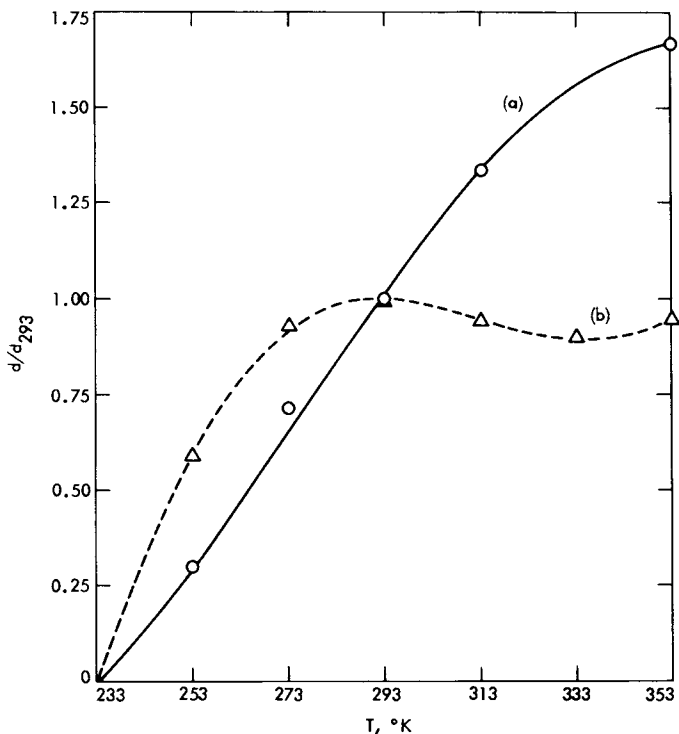


Fig. 13. Dependence of tear diameter d on temperature for series A (glass), based on (a) actual data; (b) on a hypothetical case where d is related to viscoelasticity.

all but 233°, 313°, and 333° data were used for superposition. In the remaining temperatures, other points had to be discarded for the superposition to be possible. The transformed curve is shown in Figure 10 below, and the temperature dependence of a_T in Figure 11, alongside the τ results. Despite the uncertainty at high temperatures caused by the great scatter, there is an indication of agreement with WLF. (Also of interest is the fact that the data of the filled and unfilled materials coincided in the transformed curve. This suggests that the contribution of the glass beads to strength is only through the increase of the tear diameter.)

Smith,⁹ as far back as 1958, applied the shifting technique to the stress and strain at break obtained from a simple tension test of SBR ring samples. His work was based on theory advanced by Bueche¹⁰ according to which the tensile strength for a given material is a universal function of the temperature-reduced time (or rate), the shift factor being the same as used for viscoelastic

data. Although Smith succeeded in performing a superposition, he must have resorted to a practice similar to the one employed in this work for W in order to overcome the very great scatter of his results. In principle, it must be recognized that only the quantities as measured at the tearing zone—whether stress, strain or energy—could be expected to superpose well, because only they represent true material properties.

Since it is now agreed that W_t obeys the WLF superposition, the temperature dependence of d may be deduced from the excess of shifting for τ relative to that of WLF. The details of the operation are not shown, but the final results is shown in Figure 13a where the tear diameter is presented as the ratio of the diameter at any temperature to the diameter at 293°K, the latter being the value actually measured (shown in the table).

If d is a property reflecting the viscoelastic behavior of the material, like W_t , then the shift factor for τ would be $2a_T$ and the above curve would assume the shape shown in Figure 13b. It is seen that if this was the case (which obviously it is not), the tear diameter would become practically independent of temperature above 273°K.

CONCLUSIONS

1. The stress-strain behavior of rubber obtained from a simple tension test is only a part of the total behavior as experienced by the material at the failure zone.

2. The nominal input energy density to failure is not a material property. The energy density at the tear zone is the strength-determining property.

3. The tearing energy is the second-generation material property, being dependent both on the tearing-zone energy density and on the natural tear diameter.

4. The energy density at the tearing zone is a property related to the viscoelastic behavior of the material and as such it obeys the WLF equation. The tear diameter does not obey WLF and therefore neither does the tearing energy.

5. The energy concentration at the tearing zone is highest ($k \approx 10$) for the unfilled material and lowest ($K \rightarrow 1$) for the carbon-filled material at the optimum filler level, i.e., when knots of large diameter develop.

6. The reinforcement of the SBR by carbon blacks is due to the increase of both the input energy (the intrinsic strength) and the tear diameter, with the latter being the predominant factor. For HAF, the energy reinforcement factor is about 3, and the tear-diameter reinforcement factor is 13. For MT, the corresponding figures are 1.7 and 30. The relatively small contribution of glass beads is only through the effect on the tear diameter.

7. The fluctuations in the tearing force observed during any single tearing test (even in a steady tear) are the result of the variability of the tear diameter during the test, while the intrinsic strength is almost constant.

This paper presents results of one phase of research conducted at the Jet Propulsion Laboratory, California Institute of Technology in 1968/69 during a Sabbatical leave of the first author from the Technion, Israel Institute of Technology. It was conducted under Contract No. NAS7-100, sponsored by the National Aeronautics and Space Administration. The authors wish to acknowledge the help extended by Dr. R. F. Fedors of the Jet Propulsion Laboratory.

Appendix

I. Mix Formulations (all in grams)

Series A					
Filler level ϕ (vol-%)	0	10	20	30	40
SBR-1500	1200	1100	1000	900	800
Glass beads	0	323	660	1020	1410
Dicup R	6.84	6.24	5.70	5.13	4.56

Series B					
Filler level ϕ (vol-%)	0	10	20	30	40
SBR-1500	920	870	770	673	575
MT carbon black	0	190	380	570	760
Dicup R	5.25	4.95	4.40	3.85	3.30

Series C						
Filler level ϕ (vol-%)	0	10	20	25	30	35
SBR-1500	920	870	770	906	673	730
HAF carbon black	0	190	380	594	570	770
Dicup R	5.25	4.95	4.40	5.18	3.85	4.17

II. Fillers' Physical Properties

<i>Specific gravities, g/cm³</i>		<i>Mean diameters, μ</i>	
Glass beads	2.42	Glass beads	34
Carbon black	1.80	MT	0.3
SBR-1500	0.943	HAF	0.03

References

1. R. S. Rivlin and A. G. Thomas, *J. Polym. Sci.*, **10**, 291 (1953).
2. A. G. Thomas, *J. Polym. Sci.*, **18**, 177 (1955).
3. H. W. Greensmith, *J. Appl. Polym. Sci.*, **3**, 183 (1960).
4. J. Glucklich, Technion R & D Found. Report TDM 71-06, 1971.
5. G. J. Lake, P. B. Lindley, and A. G. Thomas, 2nd International Conference on Fracture (Brighton), Paper 43, 1968, p. 493.
6. A. N. Gent and A. W. Henry, *Proc. Inst. Rubber Ind.*, 193 (1967).
7. L. Mullins, *Trans. Inst. Rubber Ind.*, **35**, 213 (1959).
8. J. D. Ferry, *Viscoelastic Properties of Polymers*, 2nd ed., Wiley, New York, 1970.
9. T. L. Smith, *J. Polym. Sci.*, **32**, 99 (1958).
10. F. Bueche, *J. Appl. Phys.*, **26**, 1133 (1955).

Received March 6, 1975

Revised May 14, 1975